

Determination of Hydraulic Conductivity Using a Modified Cylindrical-Half-Spherical Piezocone Model

Mingfei Zhang^{1,2} · Li-yuan Tong^{1,2}

Received: 25 August 2016 / Revised: 13 January 2017 / Accepted: 17 January 2017 / Published online: 21 February 2017
© Iran University of Science and Technology 2017

Abstract To obtain more accurate values of in situ hydraulic conductivity, the present paper has outlined a new method based on the analysis and comparison of existing methods using piezocone data. Owing to results obtained from many numerical simulations and in situ tests, more substantial assumptions are proposed as being more suitable: (1) the flow surface of pore water is assumed to be cylindrical-half-spherical in shape, and (2) the negative exponential function rules the distribution of excess pore water pressure in the soil around the cone. A comparison is carried out between the proposed approach and existing methods based on the graphical and statistical analysis of test data obtained from Quaternary deposits in the Yangtze Delta region. According to the qualitative graphical analysis, the proposed method can evaluate the hydraulic conductivity of soil more accurately. Five different indices and a new graphical analysis using cumulative frequency can be utilized to assess the similar equations. In addition, the results revealed the accuracy and validity of the proposed method, with these methods. The reasonable assumptions, logical derivation, and mathematical analysis together indicate the academic value and application potential of the proposed method. This model and the graphical analysis using cumulative frequency have important guiding significance for the similar analysis.

Keywords Hydraulic conductivity · CPTU · Cylindrical-half-spherical flow model · Statistical assessment · Cumulative frequency

Abbreviations

a	Radius of the cone
B_c	The calculated $B_q Q_t$
B_m	The measured $B_q Q_t$
f_s	Sleeve friction
i_a	The hydraulic gradient at radius $r = a$
h	Height of filter ring
k	Hydraulic conductivity
k_h	Hydraulic conductivity in the horizontal direction
h_c	The hydraulic conductivity calculated from equations
h_l	The hydraulic conductivity measured directly from tests
K_D	Dimensionless hydraulic conductivity coefficient
n	The number of data points
q_t	Cone resistance
SD	Standard deviation
U	The rate of cone penetration
u_a	The absolute pore water pressure measured by the piezocone
u_s	The initial static pore water pressure
u_0	Hydrostatic pressure
u_2	Pore water pressure on the cone shoulder
ξ	A reduction factor
θ, ε	Soil parameter
μ, σ	The mean and standard deviation
σ_{v0}	The total overburden stress
σ'_{v0}	The initial vertical effective stress
ΔV	The rate of volume penetration

✉ Li-yuan Tong
atmu@seu.edu.cn; seutunnel@gmail.com

¹ Institute of Geotechnical Engineering, Southeast University, Nanjing 210096, China

² Jiangsu Key Laboratory of Urban Underground Engineering and Environmental Safety, Southeast University, Nanjing 210096, China

1 Introduction

As an economic and efficient site investigation method, the piezocone penetration test (CPTU) always provides near-continuous measurements of tip resistance, sleeve friction, and pore water pressure at the shoulder, face, or shaft of the cone [1–3]. It can also give a quantitative measurement of various soil properties in situ, such as soil stratigraphy, soil mechanical properties, soil type, and the distribution of soil saturation.

Hydraulic conductivity may influence consolidation deformation [4–6], the design of pit dewatering [7], the estimation of foundation settlement, and the analysis of soil consolidation [8–12]. Therefore, numerous researchers have been dedicated to studying methods of hydraulic conductivity measurement [13–25].

Generally speaking, there are three types of methods to describe the hydraulic conductivity of in situ soils derived from piezocone soundings. The first approach involves applying the Soil Behaviour Index proposed by Robertson [18, 19]. The second refers to an indirect way to introduce a relation for the coefficient of consolidation of soils via the dissipation test [26–29], which is time-consuming and labour-intensive. The third involves a semi-theoretical method based on dislocation analysis, Darcy’s law, and cavity expansion theory [6, 21–25]. Elsworth and Lee [21, 22] first proposed an explicit equation on the basis of a spherical flow assumption. Subsequently, Chai et al. [6] modified the method using a half-spherical flow assumption, which can be used for normally or lightly overconsolidated clayey deposits and loose sandy deposits. Zou et al. [25] proposed an explicit equation with radial flow normal to an improved cylindrical surface. Yet, numerical simulation of piezocone dissipation tests [30–33] shows that the distribution of excess pore pressures is more suited for a combination of cylindrical and half-spherical (cylindrical-half-spherical) flow rather than simplex half-spherical flow or cylindrical flow [15, 34–36].

The aim of this paper was to apply the assumption of cylindrical-half-spherical flow and a negative exponent distribution to estimate the in situ hydraulic conductivity of soil.

2 Modification Methods

2.1 Brief Review of Elsworth’s and Chai’s Method

To evaluate the hydraulic conductivity directly from piezocone data, Elsworth and Lee [21] first presented a spherical flow method (hereafter referred to as Elsworth’s method) based on a dislocation model [37]. To improve the accuracy of the model, Chai et al. [6] proposed a half-spherical flow

approach (hereafter described as Chai’s method), as shown in Fig. 1.

The following assumptions are essentially adopted (Fig. 1): (1) during piezocone penetration, ‘dynamic steady’ semi-spherical flow of pore water will form around the tip of the cone; (2) excess pore water pressure around the cone has a distribution of power function for radial distance; and (3) the rate of half-spherical flow of pore water through the periphery of the cavity is linearly proportional to the rate of volume penetration of the cone [38].

The hydraulic gradient at radius $r = a$ may be deduced by way of

$$i_a = \frac{1}{\gamma_w} \frac{du}{dr} \Big|_{r=a} = \frac{u_a - u_s}{a\gamma_w} = B_q Q_t \frac{\sigma'_{v0}}{a\gamma_w} \tag{1}$$

where B_q and Q_t are the dimensionless pore water pressure ratio and dimensionless tip resistance, respectively [39]:

$$B_q = (u_2 - u_0)/(q_t - \sigma_{v0}) \tag{2}$$

$$Q_t = (q_t - \sigma_{v0})/(\sigma'_{v0}). \tag{3}$$

Half-spherical radial flow around the cone per unit time can be obtained using the following equation:

$$q = 2\pi a^2 i_a k. \tag{4}$$

Cone penetration amount per unit time is given by the following equation:

$$\Delta \dot{V} = \pi a^2 U. \tag{5}$$

Substituting Eq. (1) into Eq. (4), and assuming $\Delta \dot{V} = q$, one can obtain the following equation:

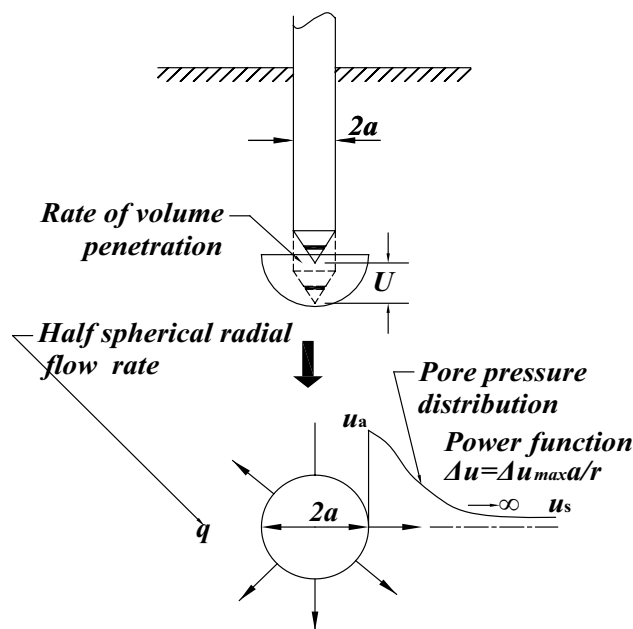


Fig. 1 Basic concept of Chai’s method (modified from [6])

$$2kB_qQ_t \frac{\sigma'_{v0}}{a\gamma_w} = U. \tag{6}$$

If a dimensionless hydraulic conductivity coefficient $K_D = 1/B_qQ_t$ was introduced, Elsworth’s method [21] first gave a bi-linear relation:

$$K_D = \begin{cases} 1/B_qQ_t, B_qQ_t < 1.2 \\ 0.62/(B_qQ_t)^{1.6}, B_qQ_t > 1.2 \end{cases} \tag{7}$$

And then, Chai et al. [6] modified this in terms of another bi-linear relation defined by the following:

$$K'_D = \begin{cases} 1/B_qQ_t, B_qQ_t < 0.45 \\ 0.044/(B_qQ_t)^{4.91}, B_qQ_t > 0.45 \end{cases} \tag{8}$$

2.2 Zou’s Method

Considering half-spherical flow may be more suitable for pore water pressure on the cone shoulder, Zou et al. [25] proposed an explicit equation (see Fig. 2a), assuming radial flow normal to an improved cylindrical surface, which is given by the following equation:

$$K''_D = \begin{cases} 1/B_qQ_t, B_qQ_t < 0.35 \\ 0.017/(B_qQ_t)^{4.64}, B_qQ_t > 0.35 \end{cases} \tag{9}$$

3 The Improved Method

To determine the distribution of initial excess pore water pressure during penetration near the cone tip more precisely, a number of laboratory, field tests (Fig. 3), and numerical simulations (Fig. 4) were carried out. The results derived from Fig. 3 revealed that the negative exponent distribution of the initial excess pore water pressure near the tip could fit the test results more closely [15, 34–36]. In addition, the results obtained from Fig. 4 indicated that the surface area for water flow seems to be more half-spherical–cylindrical in shape. Hence, the improved cylindrical–half-spherical flow assumptions are described as follows (see Fig. 2b).

The diameter of the cylindrical and half-spherical cavity is assumed to be the same as the diameter of the cone.

The height of the cylindrical cavity is assumed to be the height of the cone.

The negative exponential function rules the distribution of excess pore water pressure in the soil around the cone.

Based on the assumption $q = \Delta \dot{V} (= \pi a^2 U)$, the mathematical function adopted in this case is as follows:

$$2\pi a \cdot h \cdot k_h \cdot i_a + 2\pi a^2 \cdot k_h \cdot i_a / \xi = \pi a^2 U = \Delta \dot{V} \tag{10}$$

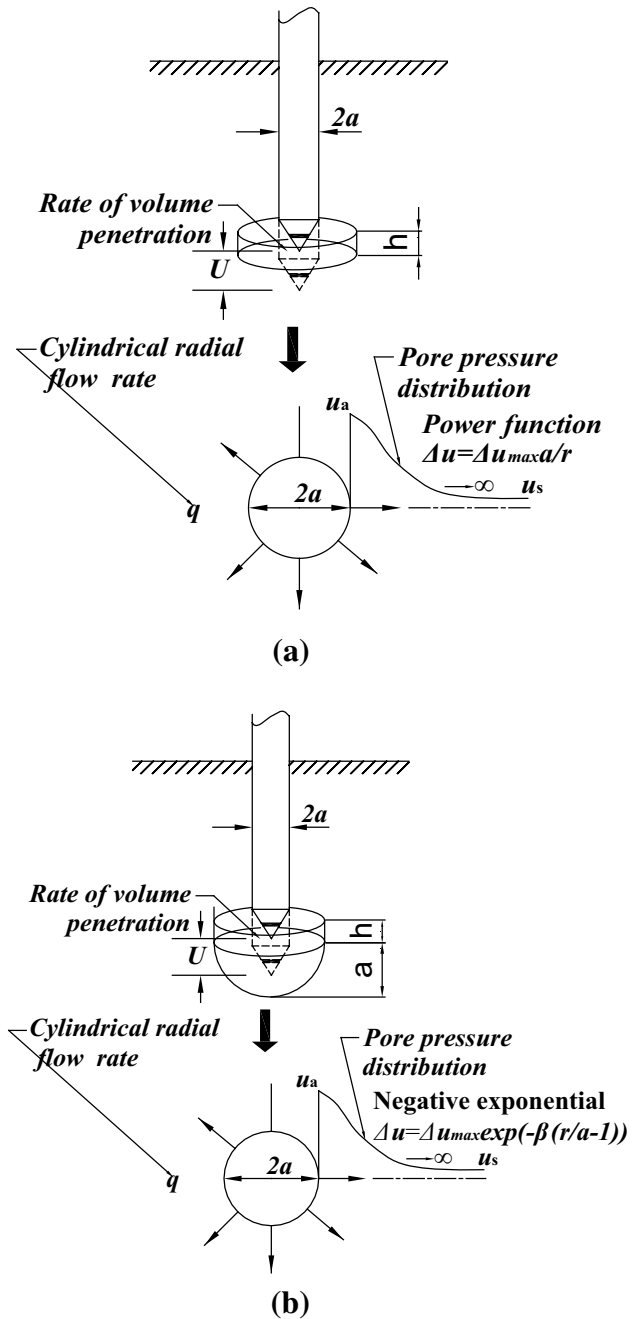


Fig. 2 Basic concept behind: **a** Zou’s method [25]; **b** the method proposed in the present paper

where ξ is a reduction factor of the half-spherical cavity determined by tests and simulations, because for the conventional CPTU, the surface area for water flow seems to be more half-spherical–cylindrical in shape near the cone and cylindrical–half-spherical in shape around the cone at larger scales than half-spherical or spherical (Fig. 4).

In addition, assuming that excess pore water pressure is zero for radial distance $r \rightarrow \infty$, the distribution of pore water pressure u can be expressed as follows:

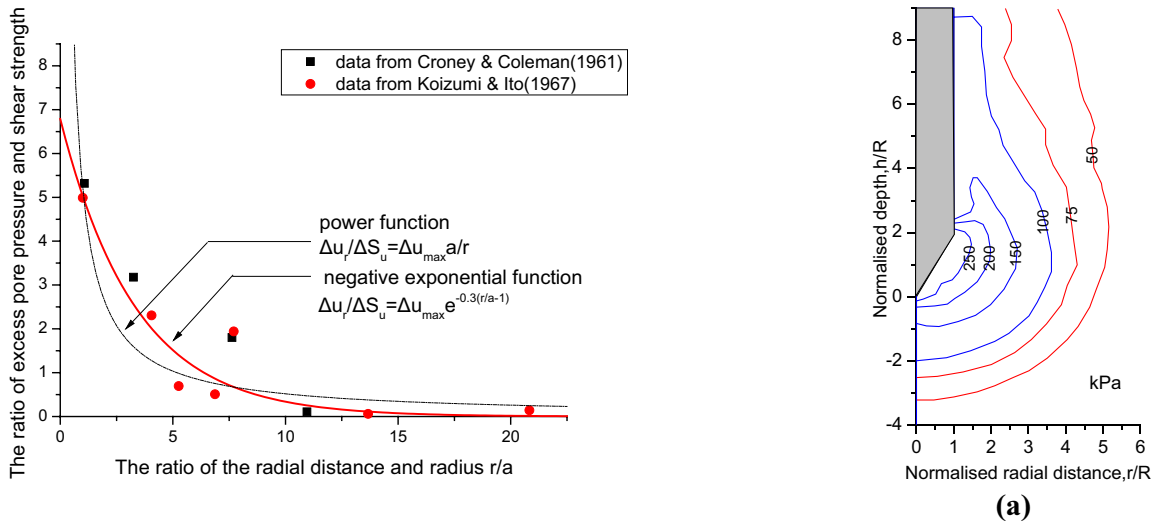


Fig. 3 Fitting curve between the initial pore water pressures with negative exponent distribution (modified from Wang et al. [24])

$$u - u_s = (u_2 - u_s)e^{-\theta(r/a-1)} \tag{11}$$

where $0.35 < \theta \leq 1.5$ for clay, $0.3 < \theta \leq 0.35$ for silt, and $0.1 < \theta \leq 0.3$ for sand [34, 38, 41]. According to Darcy’s law, i_a can be given by

$$i_a = \theta \frac{u_2 - u_s}{a\gamma_w} e^{-\theta(r/a-1)} \Big|_{r=a} = \theta B_q Q_t \frac{\sigma'_{v0}}{a\gamma_w} \tag{12}$$

Moreover, Chai et al. [6] considered that K_D or k deduced from CPTU tests mainly represent the hydraulic conductivity of a natural deposit in the horizontal direction.

Substituting Eq. (12) into Eq. (10), one can obtain the following equation:

$$2(h + a/\xi) \cdot k_h \cdot B_q Q_t \theta \cdot \frac{\sigma'_{v0}}{a\gamma_w} = Ua \tag{13}$$

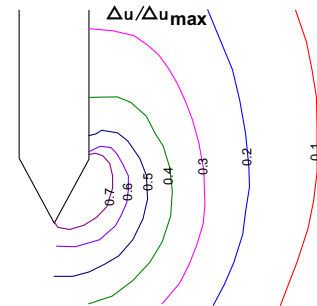
Defining $K_{D1} = 1/B_q Q_t$, one can obtain

$$K_{D1} = \frac{(h + a/\xi)\theta}{2a} \cdot \frac{4k_h \sigma'_{v0}}{Ua\gamma_w} \text{ or } k_h = \frac{2a}{(h + a/\xi)\theta} \cdot \frac{K_{D1} Ua\gamma_w}{4\sigma'_{v0}} \tag{14}$$

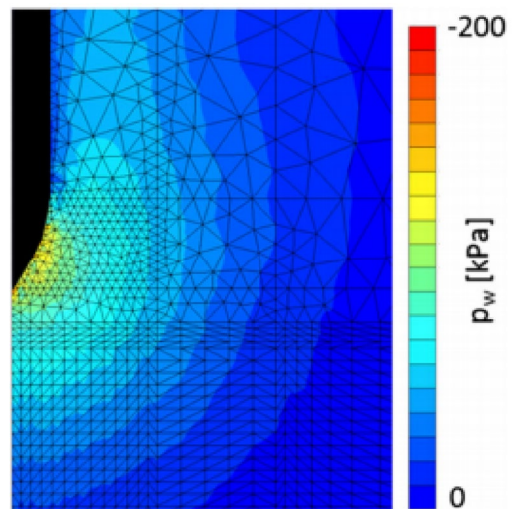
Based on the previous methods, it follows that

$$K_{D1} = \begin{cases} 1/B_q Q_t, B_q Q_t < \varepsilon \\ \alpha/(B_q Q_t)^\beta, B_q Q_t > \varepsilon \end{cases} \tag{15}$$

According to international standards for CPTU cones, their height and radius of filter ring should be equal to 5 and 17.85 mm, respectively. Considering that Ma et al. [41] suggested that the value of θ was 0.3, the data provided by [22] (see Fig. 5) can be employed to obtain values of $\xi = 2$ and $\varepsilon = 0.9$. Equation (17) can then be expressed as follows:



(b)



(c)

Fig. 4 Distribution of excess pore pressures: **a** Yi et al. [40]; **b** Mahmoodzadeh et al. [32]; **c** Ceccato and Simonini [33]

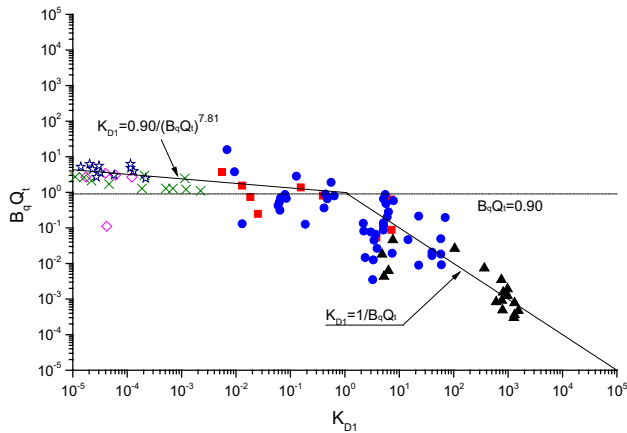


Fig. 5 Relationship between the proposed bi-linear $K_{D1} - B_q Q_t$ (data from [22])



Fig. 6 Map of the CPTU sites

$$K_{D1} = \begin{cases} 1/B_q Q_t, B_q Q_t < 0.9 \\ 0.9/(B_q Q_t)^{7.81}, B_q Q_t > 0.9 \end{cases} \quad (16)$$

4 Data

The seven sites selected for this study locates at the three cities in the eastern part of China, as shown in Fig. 6. A summary description of these sites is also provided in Table 1. Typical profiles of CPTU measurements, including cone tip resistance (q_t), side friction resistance (f_s), and pore water pressure (u_2), versus depth recorded at Hongzhuang Station in Suzhou are presented in Fig. 7. Soil samples were collected by means of a stationary piston sampler, 76 mm in diameter, at 1.0-m intervals below ground level. Once the stationary piston sampler was withdrawn from the borehole, the soil at both ends of the tube was excavated for wax sealing. Horizontal permeability tests were carried out in the laboratory on undisturbed samples of cohesive soils obtained from high-quality thin-wall samplers, with field pumping tests also performed in boreholes located on cohesionless soils. Groundwater tables at the sampling sites are located at 0 to 5 m and with depths ranging from 12 to 40 m.

The CPTU device in the study was produced by Vertek-Hogentogler and Co, USA, and comprised a versatile piezocone system equipped with advanced digital cone penetrometers fabricated with a 60° tapered, 10-cm² tip area cone, which provided measurements of q_t, f_s , and u_2 with a 5-mm-thick porous filter located just behind the cone tip. The rate of penetration for all tests was 20 mm/s, enabling one set of readings to be obtained for every 50-mm penetration.

Table 1 Soil properties and description of sites

Site name	Major soil layer	Depth range (m)	Site name	Major soil layer	Depth range (m)
Yushan Station (Suzhou)	Clay	1.0–4.8	Xinghui Road Station (Suzhou)	Clay	2.0–11.8
	Clay-rich silt	5.5–7.0		Silty sand	12.0–18.5
	Silty clay	18.6–22.4		Silty clay	19.5–28.6
Hongzhuang Station (Suzhou)	Clay	0.8–3.8	Zhuhui Road Station (Suzhou)	Clay	1.7–4.9
	Silty clay	5.5–13.6		Silt	11.0–16.8
	Silty sand—rich Silty clay	21.2–28.0		Silty clay	16–22.6
Jiangbei work well (Nanjing)	Silty clay	2.3	The fourth Yangtze River Bridge (Nanjing)	Silty clay	1.2–4.1
	Muddy clay	8–10		Silty sand	6.2–9.8
	Clay	16–18		Silty sand	16.5–18.4
The Yangtze Bridge at Taizhou (Taizhou)	Muddy clay	0.8–1.8			
	Silty clay	3.1–13.4			
	Silty sand	18.1–28.6			

Fig. 7 Typical CPTU soundings recorded at Zhuhui Station, Suzhou

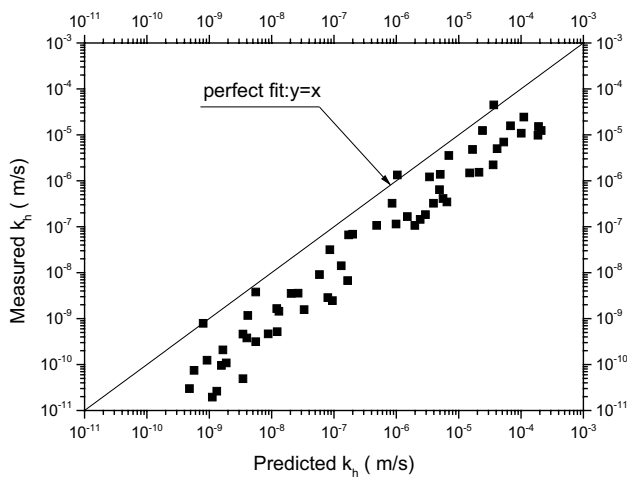
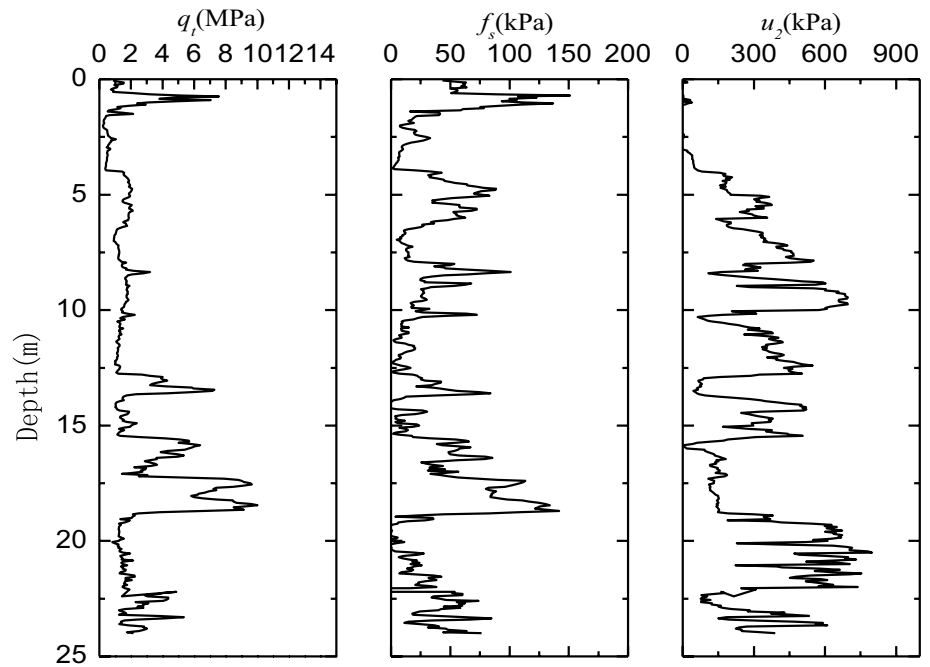


Fig. 8 Measured versus predicted k_h values for Elsworth's method

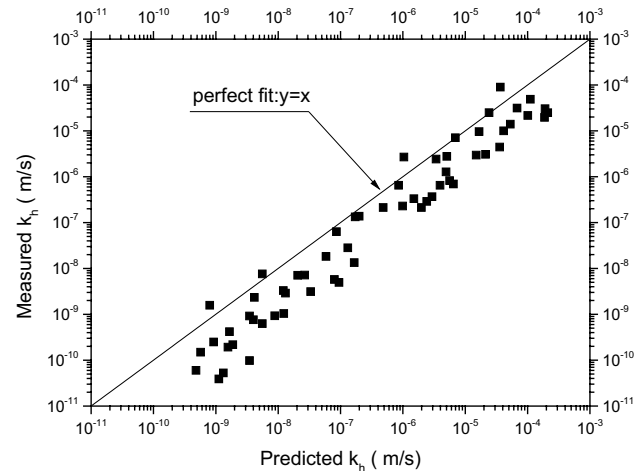


Fig. 9 Measured versus predicted k_h values for Chai's method

5 Analysis and Discussion

5.1 Qualitative Analysis

The hydraulic conductivity of soils obtained using the different CPTU interpretation methods is indicated in Fig. 8 through Fig. 15, compared with the laboratory and field pumping results. The fact that more than most of the data points are scattered below the perfect line (see Figs. 8, 9) shows that Elsworth's method and Chai's method underestimate the hydraulic conductivity of saturated soils substantially. In addition, about 60% of the data points using Zou's

method below the perfect line shown in Fig. 10 imply that the predicted accuracy of this particular method is higher than the first two methods. However, as can be seen from Fig. 11, the data points are evenly scattered around the perfect line $y=x$, which implies that the proposed method is most suitable for Yangtze Delta soils.

5.2 Quantitative Analysis

In this paper, five indexes are adopted to assess the reliability of these four above-mentioned methods: root-mean-square error (RMSE) [42–45], the first (mean) and second moments

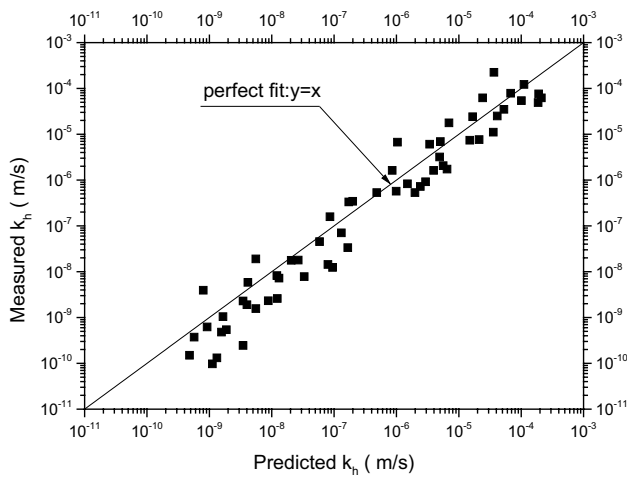


Fig. 10 Measured versus predicted k_h values for Zou’s method

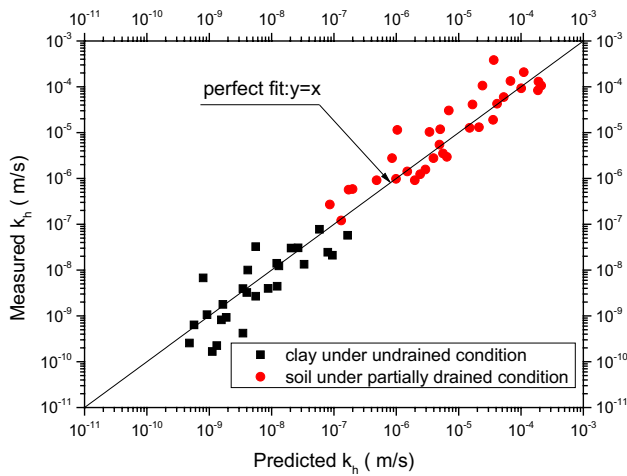


Fig. 11 Measured versus predicted k_h values for the modified method

(standard deviation SD) statistics of the ratio of the estimated to test-determined k (K), ranking index (RI) [46], ranking distance (RD) [47], and relative error index (RE).

$RMSE$ is determined via the following equation:

$$RMSE = \sqrt{\frac{1}{n} \sum_{i=1}^n (h_i - h_c)^2} \tag{17}$$

The first (mean μ) and second moment (SD standard deviation σ) statistics of the ratio of the estimated shear wave velocity to the measured shear wave velocity is denoted by K . It is determined using the following equation.

$$K = h_c/h_l \tag{18}$$

The ranking index (RI) is determined by:

$$RI = \left| \mu_{\ln(K)} \right| + \sigma_K^2 \tag{19}$$

Ranking distance (RD) is another method that takes into consideration the mean value and the standard deviation of all the K data. RD is given by [47]:

$$RD = \sqrt{(1 - \mu_K)^2 + \sigma_K^2} \tag{20}$$

RD gives equal weight to accuracy and precision, and has been used by several investigators (e.g., [48, 49]) to evaluate the performance of empirical equations.

Scaled relative error is the ratio of the difference between the measured value and the estimate to the measured hydraulic conductivity, while the absolute of it is RE . RE is mainly used to assess the pros and cons of different methods and is expressed as follows:

$$RE = |h_l - h_c|/h_l = K - 1 \tag{21}$$

The lower the $RMSE$, K , RE , RI , and RD values are, the better the correlation is.

Actually, the cumulative frequency curve is always applied to the particle-size distribution curve. Yet, it may be used for the assessment of equations in this paper (see Fig. 12), because not only can it reveals the variation range of an equation, but it also presents the variation tendency of an equation.

6 Results and Discussion

In the following section, the data are presented in logarithmic form due to the fact that the obtained values of hydraulic conductivity varied by up to six orders of magnitude. A summary of the $RMSE$, K , RE , RI , and RD values calculated by these methods is presented in Table 2. Scaled relative errors and relative error data are shown graphically in Figs. 12 and 13, respectively.

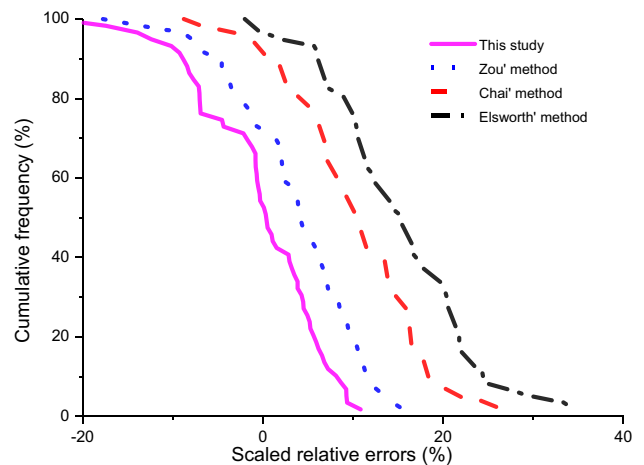
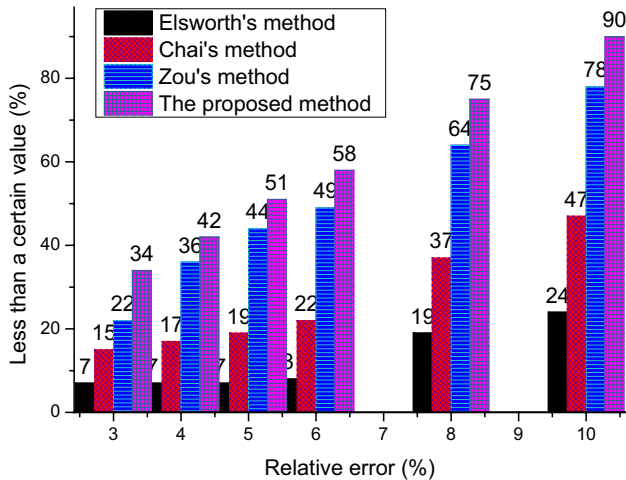


Fig. 12 Scaled relative errors of k predicted

Table 2 Results for RMSE, K , RE, RI, and RD

Methods	RMSE	K			RE			RI	RD
		>1 (%)	$ \mu $	σ	>0 (%)	$ \mu $	σ		
Elsworth's method	2.347	96.6	1.149	0.079	96.6	0.149	0.076	0.206	0.168
Chai's method	1.744	89.8	1.100	0.073	89.8	0.100	0.062	0.161	0.124
Zou's method	1.121	71.2	1.034	0.070	71.2	0.034	0.041	0.101	0.078
The proposed method	0.996	52.5	0.996	0.070	52.5	-0.004	0.045	0.066	0.070

**Fig. 13** Results for relative error RE

In terms of RMSE, the proposed method performs best (RMSE=0.996). with respect to general overestimation ($K > 1$), the percentage of the K values greater than 1 for all methods is all above than 50%, indicating that these methods all underestimate the hydraulic conductivity of soils. In terms of accuracy, the proposed method again provides the most accurate evaluation, with a K mean of 0.996. Similarly, regarding RI values, as well as the σ of K and RE, this method produces the best performance (RI=0.066). Compared to RMSE and RI, RD, which gives equal weight to accuracy and precision, is a better parameter with which to compare the suitability of different correlation equations [49]. In terms of RD, the best method is the proposed method (RD=0.070). Considering a common allowable limit of relative error (ALE) of 5%, the percentage relative error less than ALE (PRELA) is shown graphically in Fig. 13 for each method, where the higher the PRELA value, the better the correlation performance. Again, the proposed method achieves the better performance (PRELA=51%), than Zou's method (44%).

These indexes are all discontinuous and indirect, and hence, new graphical analysis using cumulative frequency is carried out in this paper. It is shown from Fig. 12 that the proposed method gives the least error. In summary, the most efficient of the four methods is the proposed method in the present paper.

7 Conclusions

To obtain more accurate the in situ hydraulic conductivity of soil, the present paper has presented a new method. A comparison of the results obtained by the proposed method and existing approaches using tests in the Yangtze Delta region was carried out. Five different indices and a new graphical analysis were utilized, from which the following significant conclusions can be drawn:

1. The cylindrical–half-spherical radial flow around the cone and the negative exponent distribution of initial excess pore water pressure near the tip are more suitable for the test and numerical results.
2. According to the qualitative graphical analysis, the proposed method can evaluate the hydraulic conductivity of soil more accurately.
3. Five different indices and a new graphical analysis can be utilized to assess the similar equations.
4. The Elsworth's and Chai's method fundamentally underestimate the hydraulic conductivity of soils. Although in terms of RI and RD, both Zou's method (RI=0.101 and RD=0.078) and the newly proposed method (RI=0.066 and RD=0.070) provide more accurate evaluations, if ALE equals to 5% the proposed method achieves a percentage relative error less than ALE with a value 7% greater than that of Zou's method (at 51% and 44%, respectively). The results of new graphical analysis using cumulative frequency, the proposed method gives the least error. Generally speaking, the most efficient method is that proposed in the present paper.

Acknowledgements Much of the research work described herein was funded by the National Natural Science Foundation of China (NSFC) (Grant No. 4157020433) and Project of the National Twelve-Five Year Research Program of China (Grant No. 2012BAJ01B02). These financial supports are gratefully acknowledged.

References

1. Campanella RG, Robertson PK (1988) Current status of the piezocone test. In penetration testing 1988, Rotterdam

2. Lunne T, Robertson PK, Powell JJM (1997) Cone penetration testing in geotechnical practice. Chapman and Hall, London
3. Mitchell JK, Brandon TL (1998) Analysis and use of CPT in earthquake and environmental engineering. *Geotech Site Character* 1:69–96
4. Shen SL, Du SJ, Huang XC, Han J (2003) Laboratory studies on property changes in surrounding clays due to installation of deep mixing columns. *Mar Georesour Geotec* 21(1):15–35
5. Zeng LL, Hong ZS, Cai YQ, Han J (2011) Change of hydraulic conductivity during compression of undisturbed and remolded clays. *Appl Clay Sci* 51(1–2):86–93
6. Chai JC, Agung PMA, Hino T, Igaya Y, Carter JP (2011) Estimating hydraulic conductivity from piezocone soundings. *Géotechnique* 61(8):699–708
7. Ma L, Xu YS, Shen SL, Sun WJ (2014) Evaluation of the hydraulic conductivity of aquifers with piles. *Hydrogeol J* 22(2):371–382
8. Shen SL, Xu YS (2011) Numerical evaluation of land subsidence induced by groundwater pumping in Shanghai. *Can Geotech J* 48(9):1378–1392
9. Horpibulsuk S, Yangsukaseam N, Chinkulkijniwat A, Du YJ (2011) Compressibility and permeability of Bangkok clay compared with kaolinite and bentonite. *Appl Clay Sci* 52(1–2):150–159
10. Xu YS, Ma L, Shen SL, Sun WJ (2012) Evaluation of land subsidence by considering underground structures that penetrate the aquifers of Shanghai, China. *Hydrogeol J* 20(8):1623–1634
11. Xu YS, Shen SL, Cai ZY, Zhou GY (2008) The state of land subsidence and prediction activities due to groundwater withdrawal in China. *Nat Hazards* 45(1):123–135
12. Xu YS, Shen SL, Du YJ, Chai JC, Horpibulsuk S (2013) Modelling the cutoff behavior of underground structure in multi-aquifer-aquitard groundwater system. *Nat Hazards* 66(2):731–748
13. Randolph MF, Wroth CP (1979) An analytical solution for the consolidation around a driven pile. *Int J Numer Anal Met* 3(3):217–229
14. Clarke BG, Carter JP, Wroth CP, Clarke BG, Wroth CP (1979) In situ determination of the consolidation characteristics of saturated clays. *European Conference on Soil Mechanics and Foundation Engineering*, London
15. Baligh MM, Levadoux JN (1980) Pore pressure dissipation after cone penetration Massachusetts. Massachusetts Institute of Technology, Department of Civil Engineering, Cambridge
16. Leroueil S, Jamiolkowski M (1991) Exploration of soft soil and determination of design parameters. *Proceedings GeoCoast'91*, Yokohama
17. Cai GJ, Liu SY, Tong LY, Du GY (2007) Study on consolidation and permeability properties of Lianyungang marine clay based on piezocone penetration test. *Chin J Rock Mech Eng* 26(4):846–857 (**Chinese**)
18. Robertson PK (1990) Soil classification using the cone penetration test. *Can Geotech J* 27(1):151–158
19. Robertson PK (2009) Estimating in-situ soil permeability from CPT and CPTU. *Can Geotech J* 46(1):442–447
20. Jefferies MG, Davies MP (1993) Use of CPTU to estimate equivalent SPT N60. *Geotech Test J* 16(4):11
21. Elsworth D, Lee DS (2005) Permeability determination from on-the-fly piezocone sounding. *J Geotech Geoenviron* 131(5):643–653
22. Elsworth D, Lee DS (2007) Limits in determining permeability from on-the-fly uCPT sounding. *Géotechnique* 57(8):679–686
23. Wang JP, Xu YS, Ma L, Shen SL (2013) An approach to evaluate hydraulic conductivity of soil based on CPTU test. *Mar Georesour Geot* 31(3):242–253
24. Wang JP, Shen SL (2013) Determination of permeability coefficient of soil based on CPTU. *Rock Soil Mech* 11:3335–3339 (**in Chinese**)
25. Zou HF, Cai GJ, LIU SY (2014) Evaluation of coefficient of permeability of saturated soils based on CPTU dislocation theory. *Chin J Geotech Eng* 36(3):519–528 (**Chinese**)
26. Gupta RC, Davidson JL (1986) Piezocone determination coefficient of consolidation. *Soils Found* 26(3):12–22
27. Robertson PK, Sully JP, Woeller DJ, Lunne T, Powell JJM, Gillespie DG (1992) Estimating coefficient of consolidation from piezocone test. *Can Geotech J* 29(4):539–550
28. Danziger FAB, Almeida MSS, Sills GC (1997) The significance of the strain path analysis in the interpretation of piezocone dissipation data. *Géotechnique* 47(5):901–914
29. Burns SE, Mayne PW (1998) Monotonic and dilatatory pore pressure decay during piezocone tests in clay. *Can Geotech J* 35(6):1063–1073
30. Yi JT, Lee FH, Goh SH, Zhang XY, Wu JF (2012) Eulerian finite element analysis of excess pore pressure generated by spudcan installation into soft clay. *Comput Geotech* 42:157–170
31. Mahmoodzadeh H, Randolph M F, and Wang, D (2014) Numerical simulation of piezocone dissipation test in clays. *Géotechnique* 64(8):657–666
32. Mahmoodzadeh H, Wang D, Randolph MF (2015) Interpretation of piezoball dissipation testing in clay. *Géotechnique* 65(10):831–842
33. Ceccato F, Simonini P (2016) Numerical study of partially drained penetration and pore pressure dissipation in piezocone test. *Acta Geotech* 1–15
34. Zhu XL, Tang SD (1986) Theoretical analysis of the coefficient of consolidation in soft clay estimated by pore water pressure-cone of cone penetration test. *Geotech Investig Surv* (6):8–12
35. Zhu XR, He YH, Xu CF, Wang ZL (2005) Excess pore water pressure caused by single pile driving in saturated soft soil. *Chin J Rock Mech Eng* 24(2):725–732 (**in Chinese**)
36. Tang SD, He LS, Fu Z (2002) Excess pore water pressure caused by an installing pile in soft foundation. *Rock Soil Mech* 23(6):725–732
37. Elsworth D (1991) Dislocation analysis of penetration in saturated porous media. *J Engng Mech Div* 117(2):501–516
38. Shen SL, Wang JP, Wu HN, Xu XS, Ye GL (2015) Evaluation of hydraulic conductivity for both marine and deltaic deposits based on piezocone testing. *Ocean Eng* 110:174–182
39. Wroth CP (1984) Interpretation of in situ soil tests. *Géotechnique* 34(4):449–489
40. Yi JT, Goh SH, Lee FH, Randolph MF (2012) A numerical study of cone penetration in fine-grained soils allowing for consolidation effects. *Géotechnique* 62(8):707–719
41. Ma SZ, Tang YC, Meng GT (2007) Piezocone penetration test mechanism, methods and its engineering application. The China University of Geosciences Press, Wuhan
42. Grima MA, Babuška R (1999) Fuzzy model for the prediction of unconfined compressive strength of rock samples. *Int J Rock Mech Min* 36(3):339–349
43. Shahnazari H, Shahin MA, Tutunchian MA (2014) Evolutionary-based approaches for settlement prediction of shallow foundations on cohesionless soils. *Int J Civ Eng* 12(1):55–64
44. Abedimahzoon N, Neshaei ML (2013) Investigation of the surf zone hydrodynamics in the vicinity of reflective structures by taking the nonlinearity of waves and wave-current interactions into account. *Int J Civ Eng* 11(4A):261–271
45. Tu KJ, Huang YW (2013) Predicting the operation and maintenance costs of condominium properties in the project planning phase: an artificial neural network approach. *Int J Civ Eng* 11(4A):242–250

46. Briaud J, Tucker LM (1988) Measured and Predicted Axial Response of 98 Piles. *J Geotech Eng* 114(9):984–1001
47. Cherubini C, Orr TLL (2000) A rational procedure for comparing measured and calculated values in geotechnics. *Coastal Geotechnical Engineering in Practice, Yokohama*, 1:261–265
48. Giasi CI, Cherubini C, Paccapelo F (2003) Evaluation of compression index of remolded clays by means of Atterberg limits. *Bull Eng Geol Environ* 62(4):333–340
49. Onyejekwe S, Kang X, Ge L (2015) Assessment of empirical equations for the compression index of fine-grained soils in Missouri. *Bull Eng Geol Environ* 74(3):705–716